Title

Biocompatible sodium alginate fibers by aqueous processing and physical crosslinking

Journal

Carbohydrate Polymers, 102(1)

ISSN

0144-8617

Authors

Shen, Wei

Hsieh, You-Lo

Publication Date

2014-02-01

DOI

10.1016/j.carbpol.2013.10.066

Peer reviewed

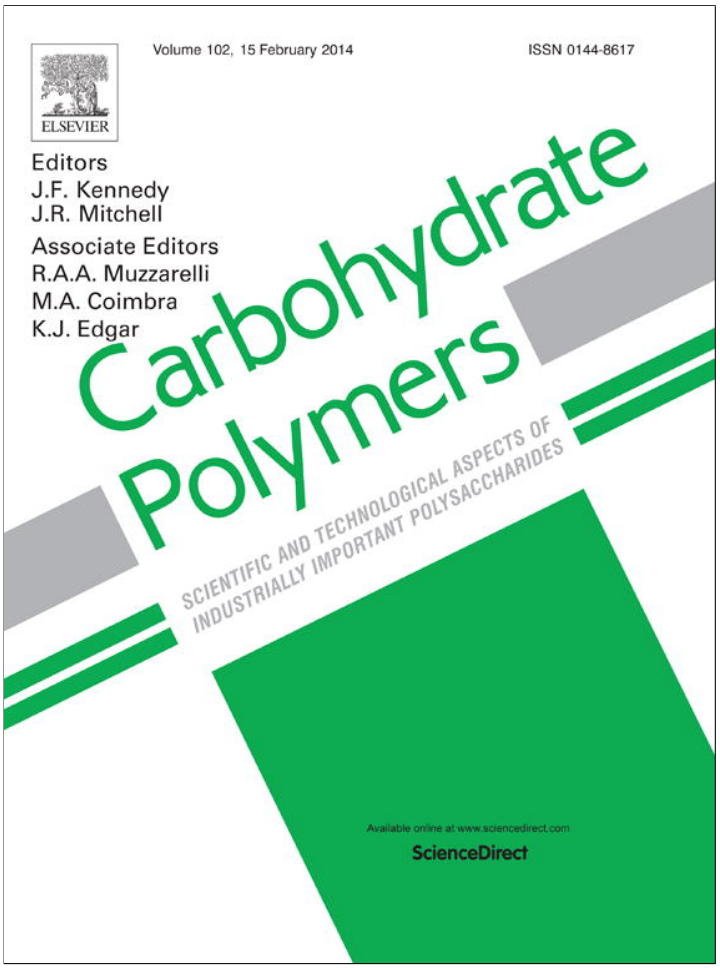

Carbohydrate Polymers 102 (2014) 893–900

Contents lists available at ScienceDirect

Carbohydrate Polymers

journal homepage: www.elsevier.com/locate/carbpol

Biocompatible sodium alginate fibers by aqueous processing and physical crosslinking

Wei Shen, You-Lo Hsieh*

Fiber and Polymer Science, University of California, Davis, CA 95616, USA

ARTICLE INFO

Article history:
Received 31 July 2013
Received in revised form 16 October 2013
Accepted 19 October 2013
Available online 27 October 2013

Keywords:
Sodium alginate
Electrospinning
Physical cross-linking
Aqueous
Green processing

ABSTRACT

Sodium alginate (SA) hybrid fibers have been robustly fabricated by electrospinning of aqueous mixtures containing as high as 60% SA in the presence of polyvinyl alcohol (PVA). Solution viscosities of SA, PVA and their mixtures showed fiber spinning to be strongly influenced by the balance between SA–PVA and PVA–PVA intermolecular polar interaction and SA–SA repulsion. Low viscosity SA_l (50 mPa s at 1%) enabled higher SA loadings without significantly increasing mixture viscosities, producing more cylindrical fibers. All aqueous mixtures containing 33.3–60% SA_l (5.68–7.15% total SA_l–PVA) had viscosities ranging from 530 to 3600 mPa s and could be electrospun continuously for at least 48 h. The SA–PVA hybrid fibers had diameters ranging from ca. 140 to 350 nm and were rendered stable in water via simultaneous ionic-crosslinking SA and crystallization of PVA (5% $CaCl_2$ in 75% EtOH for 30 min). This aqueous electrospinning and physical crosslinking approach is a green and highly efficient alternative to create alginate hybrid fibers that are biologically compatible and ingestible for potential biomedical, food and other applications.

1. Introduction

Nanofibers from electrospinning of biopolymers such as polysaccharides and proteins are of significant interest in many biological and medical applications for their high specific surface, porosity and similarity to natural extracellular matrices. Among polysaccharides, the most abundant cellulose and chitin are not soluble in water and challenging to dissolve in most organic solvents. Alginate is a readily water-soluble polysaccharide and a desirable candidate for aqueous processing. Alginate is a linear anionic polysaccharide, most commonly derived from marine brown algae. Alginate consists of two C5 epimer repeating units, i.e., (1→4)-α-L-guluronate (G) and (1→4)-β-D-mannuronate (M), which are arranged in either MM, GG or alternating GM blocks (Lee et al., 2007). The glycosidic bonds in and between these blocks lead to varied conformations along chains, i.e., linear M-blocks from the diequatorial links, bulky G-blocks from the diaxially links and irregular GM-blocks from alternating axial–equatorial glycosidic bonds.

Alginate has been widely used in tissue engineering and biomedicine for its non-toxicity, biodegradability, biocompatibility and unique gel-forming characteristics (Qin, 2004). However, aqueous alginate solutions are too viscous to be electrospun into fibers (Bhattarai, Li, Edmondson, & Zhang, 2006; Lee & Lyoo, 2009). Even at concentrations below gelation, insufficient polymer chains as well as intermolecular repulsion between anionic groups hinder chain entanglement required for fiber formation. Electrospinning of sodium alginate (SA) has only been possible from either solutions in organic solvents (Bhattarai et al., 2006; Nie et al., 2008) or aqueous mixtures containing synthetic water-soluble polymers, such as poly(vinyl alcohol) (PVA) (Islam & Karim, 2010; Lee et al., 2007; Safi, Morshed, Hosseini Ravandi, & Ghiaci, 2007; Shalumon et al., 2011) and poly(ethylene oxide) (PEO) (Alborzi, Lim, & Kakuda, 2010; Bhattarai et al., 2006; Bonino et al., 2011; Kong, Yu, Ji, & Xia, 2009; Lu, Zhu, Guo, Hu & Yu, 2006; Ma, Fang, Liu, Zhu, & Nie, 2012; Nie et al., 2009; Safi et al., 2007; Zhang, 2007). From aqueous media, uniform fibers with SA as the dominant polymer could only be electrospun from mixtures with PEO. In cases where 80% SA have been electrospun with PEO, attempts to cross-link SA/PEO fibers with $CaCl_2$ failed to retain the fiber structure which had became film-like from either crosslinking or after subsequent water immersion (Bonino et al., 2011; Lu et al., 2006; Ma et al., 2012). Electrospinning SA in aqueous mixtures with PVA, on the other hand, has produced highly beaded fibers at up to 50% SA and none crosslinked.

This objective of study was to achieve higher SA-containing fibers by efficient aqueous electrospinning as well as render SA hybrid fibers insoluble in water, while preserving biologically compatibility and ingestibility. Specifically, green processing approaches, i.e., 100% aqueous media and crosslinking by physical means, were developed to achieve these goals. SA contents

* Corresponding author. Tel.: +1 530 752 0843; fax: +1 530 752 7584.
E-mail address: ylhsieh@ucdavis.edu (Y.-L. Hsieh).

0144-8617/$ – see front matter © 2013 Elsevier Ltd. All rights reserved.
http://dx.doi.org/10.1016/j.carbpol.2013.10.066

were optimized by studying the effects of SA/PVA ratios, total SA–PVA concentrations and SA molecular weights on the viscosities and electrospinability of aqueous SA/PVA mixtures. Simultaneous cross-linking of both SA and PVA in a single process was investigated. Previously, bivalent cations, such as Ca^{2+} cation, have shown to ionically cross-link alginate to gelation (Rhim, 2004) while alcohol exchange has improved the crystallinity of PVA (Donati & Paoletti, 2009). In this work, ionic crosslinking of alginate and crystallization of PVA and simultaneous application of both to render SA/PVA fibers insoluble in water were investigated. The resulted fiber structures as well as chemical and thermal properties were characterized. These green processing approaches would lead to alginate dominant fibers that are biologically compatible and ingestible for potential biomedical, food and other applications.

2. Materials and methods

2.1. Materials

Poly (vinyl alcohol) (PVA, M_w = 146–186 kDa; 99% hydrolyzed) was purchased from Sigma–Aldrich. Two kinds of sodium alginate (SA) were used. Low viscosity sodium alginate (SA_l) and medium viscosity sodium alginate (SA_m) were purchased from Alfa Aesar and Acros Organics, respectively, and used without further purification. The G/M ratios of SA_l and SA_m were determined by NMR to be 6.6 and 3.5, respectively (supplemental information). Triton X-100 was purchased from EMD Company. Water used in this paper was purified by Milli-Q^{TM} plus water purification system.

2.2. Solutions preparation and viscosity

Aqueous solutions of pure SA_m, SA_l and PVA were prepared at 4%, 8% and 12% respectively. All concentrations were in weight % unless specified otherwise. PVA was dissolved in water under constant stirring at 95 °C for 8 h, then at ambient temperature for another 2 h to homogeneous solution. SA was dissolved in water at ambient temperature. Sequential dilutions of each solution produced varied concentrations to establish the viscosity to concentration relationship for each polymer.

Aqueous mixtures of SA and PVA were prepared at different SA/PVA mass ratios and varied total SA/PVA concentrations. SA_m/PVA mixtures were prepared by mixing individual aqueous SA and PVA solutions at ambient temperature where SA_l/PVA mixtures were made by adding solid SA_l directly into aqueous PVA solutions at 65 °C. The viscosities of aqueous PVA and SA solutions as well as their mixtures at varying concentrations and mixed ratios were measured within 24 h after their preparation using a Haake Viscotester 7 Plus viscometer. Each solution was poured into a 50 mL tube with an inner diameter of 20 mm and the viscosities were measured at the ambient temperature and reported as apparent viscosity.

2.3. Electrospinning

The electrical apparatus consisted of a high voltage power supply (Gamma High Voltage Research Inc, ES 30), a syringe, a needle tip and a collector. All the mixed solution was loaded into a 20 mL plastic syringe capped with a 24 gauge blunt needle. A positive voltage between 15 kV to 20 kV was applied to the needle to charge the solution which was fed at a 0.5 mL/h rate (KD Scientitic). The electrospun products were collected on a 40 cm square ground iron mesh collector placed ca. 20 cm from the tip of the needle. All solutions were electrospun at the ambient temperature with 0.05% Triton X-100 added.

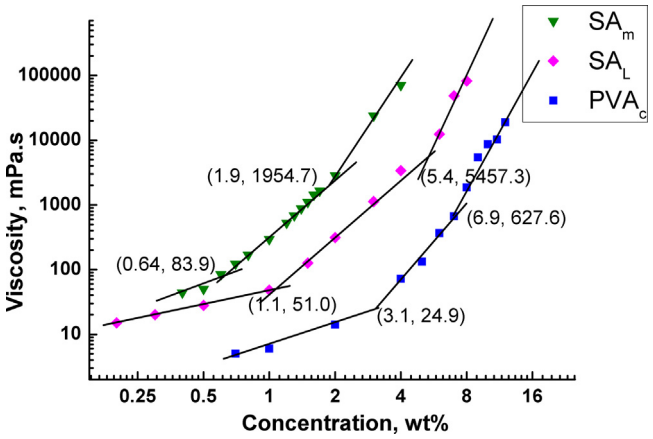

Fig. 1. Viscosity of aqueous SA_m, SA_l and PVA solutions at the ambient temperature.

2.4. Cross-linking

Different ethanol solutions were prepared for cross-linking PVA fibers electrospun from 8% aqueous solution. Ethanol solutions followed by $CaCl_2$/ethanol solutions with various Ca^{2+} and ethanol concentration were used as both alcohol exchange cross-linking and ionic cross-linking on 2% SA_m casted film cast and SA_L/PVA fibers electrospun from 5% mixture at 3/7 ratio. The extent and effect of crosslinking was examined by the stability of fibers or films in water and mass after 2 h water immersion. Mass was recorded following each step in crosslinking and after water immersion and mass change (ΔW) was calculated as:

$$\Delta W = \frac{100(W_t - W_i)}{W_i}$$

where W_i and W_t denote the initial dry weight and that of the sample after water immersion and drying at 65 °C. All the weight loses were based on original mass and reported as cummulative values.

2.5. Characterization

All samples were dried at 65 °C before being characterized. The thermal properties were measured using differential scanning calorimetry (DSC) (DSC-60, Shimadzu, Japan) and thermogravimetric analysis (TGA-50, Shimadzu, Japan). All samples were placed in crimped aluminum pans and heated at a heating rate of 10 °C/min under N_2 gas from the ambient temperature to 400 °C. The fiber morphology of the fibrous web structure was examined using an optical microscope (Leica DM 2500) and a scanning electron microscope (SEM) (XL30-SFEG, FEI/Philips, USA), the latter at an accelerating voltage of 15 kV after sputter-coating the specimens with Au. The atomic compositions of SA_l and SA_m were carried out by energy-dispersive X-ray spectroscopy (EDX) adjunct to the SEM. Fourier transform infrared spectroscopy (FT-IR) (Nicolet 6700 FTIR spectrometer) was performed between 500 and 4000 cm^{-1} on ground samples in KBr pellets.

3. Results and discussion

3.1. Solution viscosity

Both SA_m and SA_L dissolved in water in less than a minute while homogeneous aqueous PVA solution was obtained by constant stirring at 95 °C for 8 h, followed by additional 2 h at the ambient temperature. For each aqueous series, the apparel viscosities increased with increasing concentrations (Fig. 1). The distinct slope changes separate the viscosity–concentration relationship

Table 1
Viscosity (mPa s) of SA_m/PVA mixtures (based on 4% PVA) at ambient temperature.

Conc. (%)	SA_m/PVA (w/w ratio)	η measured (mPa s)	η calc. sum (mPa s)
4.19	0.48/9.52	185	109
4.38	0.91/9.09	382	115
4.57	1.30/8.70	670	116
4.76	1.67/8.33	1231	239
4.95	2/8	1859	366
5.14	2.31/7.69	3928	596
5.33	2.59/7.41	4562	870
5.51	2.86/7.14	5443	1400
5.70	3.10/6.90	6697	1820
5.88	3.33/6.67	7881	2822

into three regions: semi-dilute unentangled, semi-dilute entangled and concentrated (de Gennes, 1979). Fiber formation from spinning either polymer solutions or melts requires chain entanglement. Base on these viscosity profiles, the concentration ranges in which chain entanglements expected to occur are 0.6–1.9%, 1.1–5.4% and 3.1–6.9% for SA_l, SA_m and PVA, respectively. The viscosities for these chain entanglement concentration ranges are 51.0–5457 mPa s, 83.9–1954 mPa s and 24.9–627 mPa s for SA_l, SA_m and PVA, respectively.

Electrospinning of either aqueous SA_l or SA_m solutions in their respective entanglement concentration ranges only produced droplets, however. This is consistent with prior observations by others stated earlier. Aqueous PVA solutions in the 5–8% concentration range were electrospun into uniform fibers while those in the 1–4% range produced strings of droplets. These fiber-forming PVA concentrations had viscosities ranging from 132 mPa s to 1860 mPa s and corresponded to the upper semi-dilute entangled region to the lower concentrated region. Fibers electrospun from the 8% PVA were most uniform, but also the thickest.

3.2. Electrospinning and fiber formation of SA_m/PVA

Three series of aqueous SA_m/PVA mixtures were made by adding SA_m (from 0.08 to 0.8 g at an increment of 0.08 g) into aqueous PVA at three fixed concentrations of 2, 4 and 8% that spanned beyond its semi-dilute entangled 3.1–6.9% range at both ends. In 8% PVA, SA_m could only be dissolved at up to 1% to give a 1.1/8.9 SA_m/PVA mixture. With 2% and 4% PVA, homogenous mixtures containing up to 1.96% SA_m were obtain corresponding to 5/5 and 3.55/6.45 SA_m/PVA ratios, respectively. The highest SA_m contents were 50%, 35.5% and 11% in mixtures with 2, 4 and 8% PVA, respectively. To focus on SA contents higher than what was reported by others, only mixtures based on 2% and 4% PVA were evaluated for electrospinning.

Electrospinning of all SA_m/PVA mixtures based on 2% PVA produced only droplets. At the highest 50% SA content, the 3.92% SA_m/PVA mixture was too viscous (6637 mPa s) to be electrospun into jets. All mixtures with 4% PVA, on the other hand, could be electrospun into fibers, but with different levels of uniformity, some with droplets and beads. Therefore, the most electrospinnable mixtures based on 4% PVA were further studied.

The mixtures based on 4% PVA contained 0.79–1.96% of SA_m, or at 1.67/8.33 to 3.33/6.67 SA_m/PVA ratios, and had viscosities spanning from 1231 mPa s to 7881 mPa s (Table 1). The viscosity of these SA_m/PVA mixtures were far higher than the sums of the individual SA_m and PVA solutions at corresponding concentrations. The three to five time higher viscosities than those calculated from the individual components indicate intermolecular interactions between SA_m and PVA likely via hydrogen bonding among the abundant SA_m hydroxyls and carboxyls and PVA hydroxyls. The fiber-forming ability of these mixtures suggests that PVA chains entangle not only with each other, but also with SA_m or enhanced SA_m–PVA chain entanglement.

Table 2
Viscosity (mPa s) of SA_L/PVA mixtures at fixed ratios at ambient temperature.

Conc. (%)	SA_L/PVA (w/w ratio)	η measured (mPa s)	η calc. sum (mPa s)
5.68	3.55/6.45	1240	374
6.50	3.55/6.45	1890	648
6.80	3.55/6.45	3600	742
8.55	3.55/6.45	3510	1196
6.00	4.00/6.00	530	698
6.50	4.00/6.00	850	870
7.00	4.00/6.00	1040	1047
7.80	4.00/6.00	1500	1509
6.50	5.00/5.00	1070	1739
7.00	5.00/5.00	1430	2373
7.69	5.00/5.00	2640	3115
5.50	6.00/4.00	600	1823
6.00	6.00/4.00	1000	3118
6.50	6.00/4.00	1270	2965
7.15	6.00/4.00	1750	4730

Fibers electrospun from SA_m/PVA mixtures at a fixed 5% total concentration and different SA_m/PVA ratios were examined by SEM (Fig. 2). Electrospinning mixtures at 4/6 and higher SA_m/PVA ratios produced only droplets. Fibers electrospun from the mixture with a slightly lowered SA_m/PVA ratio of 3.33/6.67 were observed with some spindle-shape and round beads. At 3/7 SA_m/PVA ratio, electrospinning was significantly improvement as evident by cyclindrical fibers and much fewer beads. Finer and more uniform fibers, with diameter ranging from 153 nm and 260 nm and essentially no beads, were observed at a further decreased 2/8 SA_m/PVA ratio. These SEM observations show improved fiber uniformity and reduced beaded structure with decreasing SA_m contents from 33.3 to 20% in the mixtures, all continuous up to 48 h, thus with good electrospinning efficiency.

3.3. Electrospinning and fiber formation of SA_l/PVA

To further increase SA contents without increasing solution viscosity, lower viscosity SA_l was mixed with 4% PVA at several levels. Direct dissolution of SA_l solid into aqueous PVA was very slow at ambient temperature, taking days to reach over 40% SA_l. Increasing temperature to 65 °C accelerated dissolution and lowered dissolution time to 8 h.

The 4% aqueous PVA has a viscosity of 72 mPa s. Adding SA_l to 4% PVA dramatically increased the viscosities of all SA_l/PVA mixtures. At each fixed SA_l/PVA ratio, viscosities also increased with total polymer concentrations. It was interesting to note that the relationships between the viscosities of mixtures and the summation of corresponding SA_m and PVA solution viscosities were different at varied SA_l/PVA ratios (Table 2). At 3.55/6.45 SA_l/PVA ratio, the measured viscosities were much higher than the calculated sums of individual components. The measured and calculated viscosities were almost the same for 4/6 SA_l/PVA mixtures whereas the measured viscosities were much lower than the calculated sums for 5/5 and 6/4 SA_l/PVA mixtures. This could be explained by balance between SA–SA repulsion and SA–PVA interaction. The viscosity of the mixture is below the sum of individual components when the SA–SA repulsion exceeds the SA–PVA and PVA–PVA hydrogen bonding effects whereas the mixture viscosity exceeds the sum with the opposite. The repulsion and hydrogen bonding appear to be balanced at 4/6 SA_l/PVA ratio whereas hydrogen bonding dominates in mixtures containing less than 40% SA, being SA_l (Table 2) or SA_m (Table 1).

Nevertheless, all SA_l/PVA mixtures at 3/7 to 6/4 ratios (Table 2) could be electrospun into fibers continuously for more than 48 h, producing thick fibrous mats that were easily detachable from the

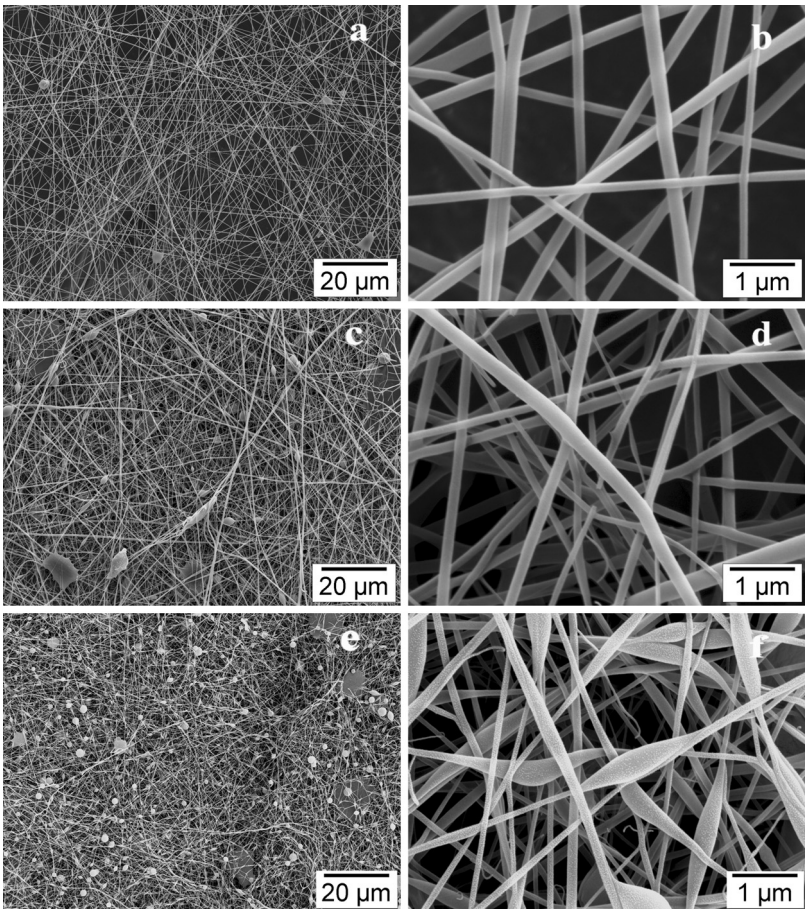

Fig. 2. Scanning electron micrographs of fibers electrospun from 5% aqueous SA_m/PVA mixtures at ratios of: (a, b) 2/8, (c, d) 3/7, (e, f) 3.33/6.67.

target and strong enough to handle. These SA_l/PVA mixtures at total concentrations between 5.68 and 7.15% fell in the 530–3600 mPa s viscosity range. Most uniform fibers without beads were produced from the 3/7 SA_l/PVA mixture (Fig. 3a and b). At a slightly higher 3.55/6.45 SA_l/PVA ratio, few beads appeared along fibers (Fig. 3c and d). Fiber sizes and increasing numbers of micrometer sized beads were observed as SA_l/PVA ratio increased to 4/6 (Fig. 3e and f) and 5/5 (Fig. 3g and h). Further raising SA_l/PVA ratio to 6/4, fibers became more irregularly shaped and few ca. 15 μm size beads were found between fibers (Fig. 3i and j).

The above observations show that both medium and low viscosity SA can be continuously electrospun into SA–PVA hybrid fibers at up to 30% SA contents. At the same 3/7 SA/PVA composition (5%), fibers electrospun from SA_l were more cylindrical with narrower size distribution and fewer beads than the SA_m counterparts. Thick fibrous mats could be robustly electrospun from mixtures containing 30% to 60% SA_l. Most significantly, fibers with 60% SA could be robustly electrospun with the lower viscosity SA_l for the first time, the highest SA content to date.

3.4. Structure and properties of ES SA/PVA fibers

FTIR spectrums of hybrid fibers electrospun from aqueous SA_m/PVA and SA_l/PVA mixtures at various ratios showed essentially PVA and SA characteristic peaks in their relative proportions (Fig. 4), i.e., PVA characteristic peaks of CH_2 stretching at 2938 cm^{-1}, CH—OH bending at 1570 cm^{-1} and 1438 cm^{-1}, C—O vibration at 1092 cm^{-1} and OH stretching at 3370 cm^{-1} and SA characteristics peaks of OH stretching at 3410 cm^{-1}, CH_2 stretching at 2927 cm^{-1} and asymmetric and symmetric —COO— stretching at 1612 cm^{-1} and 1414 cm^{-1}, respectively. The major change was the PVA CH—OH bending signal at 1570 cm^{-1}. With increasing SA_m or SA_l contents, the PVA CH—OH bending signal at 1570 cm^{-1} disappeared, possibly due to increasing inter-molecular PVA–SA hydrogen bonding.

Both SA_l and SA_m exhibited similar thermal profiles, but SA_l had smaller moisture and decomposition exotherm, latter also at slightly lower temperature range (193–254 °C, 236 J/g) comparing to SA_m (204–263 °C, 419 J/g) (Fig. 5a). The onset temperature of decomposition for SA_l was nearly 20 °C lower than that of SA_m, possibly reflecting their difference in molecular chain lengths. Both SA_l and SA_m left about 48% char at 350 °C. Electrospun PVA_c fibers exhibited a broad endotherm between 42 °C and 112 °C, from overlapping moisture estimated at 8.7% (Fig. 5b) with glass transition, reported at 85 °C. A sharp melting peak at 228.4 °C was immediately followed by a large decomposition at 298 °C that corresponded to another 53% mass loss from 217 °C to 302 °C.

The thermal behavior of SA/PVA fibers electrospun from mixtures of varied ratios showed nearly indistinguishable decomposition of SA while both melting and decomposition endotherms of PVA significantly reduced in sizes and temperatures (Fig. 6). With increasing SA_m content, PVA melting peaks lowered from 228 °C to 222 °C then 220 °C for 0/10 to 2/8 and 3/7 SA_m/PVA, respectively, while the melting endotherms significantly decreased from 55 J/g to 15 J/g then 8 J/g, indicating reduced crystalline PVA domains in the hybrid fibers. The decomposition temperature of PVA also decreased from 298 °C to 270 °C, then to 264 °C while the heat of decomposition decreased from 719 J/g to 489 J/g, then 442 J/g with increasing SA_m contents from 0 to 20% then 30%. For SA_l/PVA fibers, PVA melting peaks lowered from 228 °C to 218 °C and then

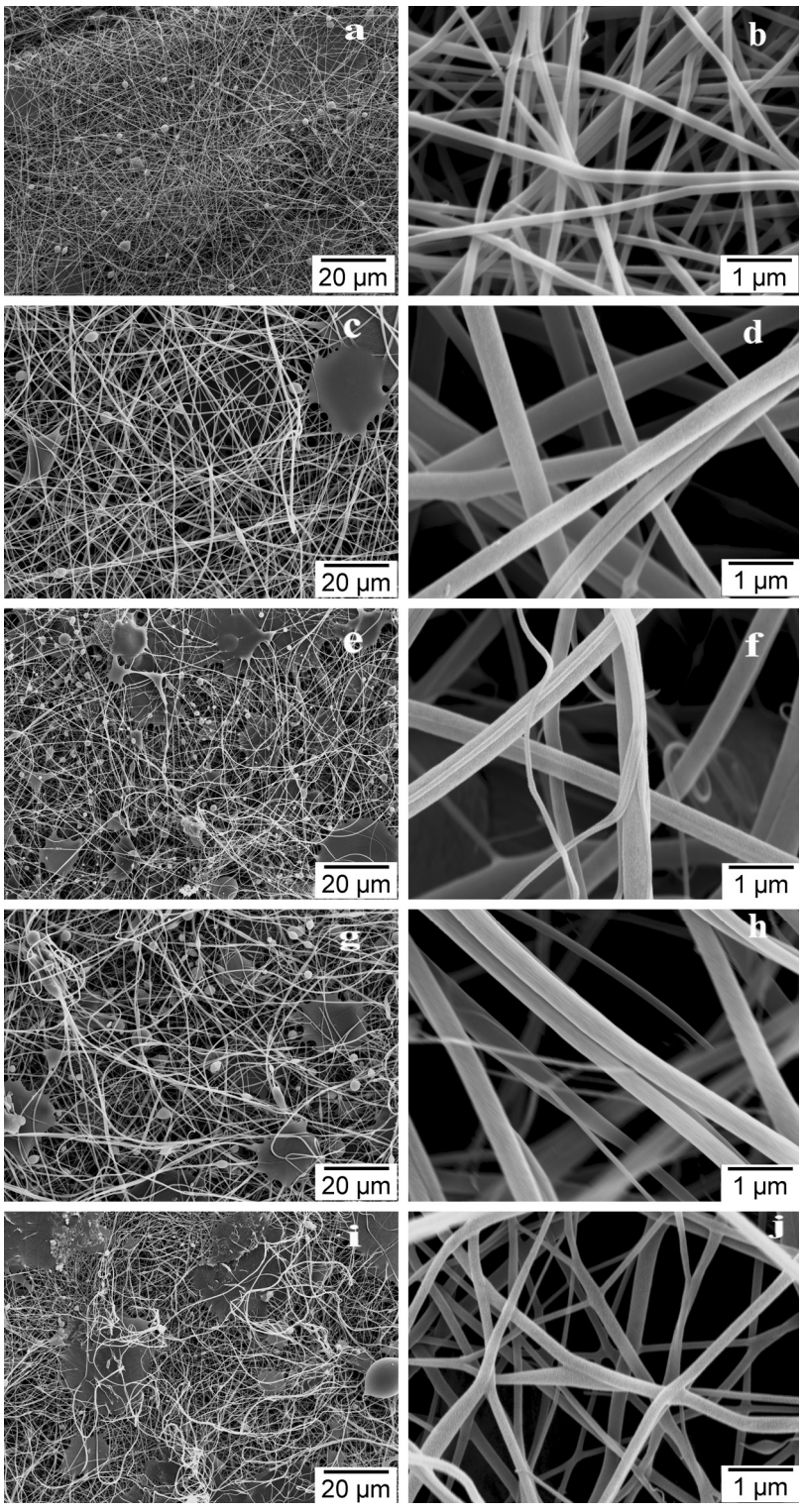

Fig. 3. Scanning electron micrographs of electrospun fibers at SA_l/PVA ratios (total conc.) of: (a, b) 3/7 (5%), (c, d) 3.55/6.45 (8.5%), (e, f) 4/6 (7.8%), (g, h) 5/5 (7.7%), (i, j) 6/4 (7.2%).

back to ca. 225 °C, while the melting end other lowered significantly from 55 J/g for PVA to 9 J/g, 11 J/g and 15 J/g for 3/7, 4/6 and 6/4 SA_l/PVA hybrid fibers. In both SA_l and SA_m hybrid fiber series, PVA melting and decomposition peaks, although considerably reduced in sizes and temperatures, still existed, indicating some PVA to be phase separated from SA. The DSC of all three SA_l/PVA fibers showed exotherms in between the PVA melting and decomposition peaks, suggesting some SA_l may also be phase separated.

3.5. Cross-linking of SA/PVA fibers

To render the SA_l/PVA hybrid fibers insoluble in water, crosslinking by alcohol exchange of PVA and ionic cross-linking of SA_l with

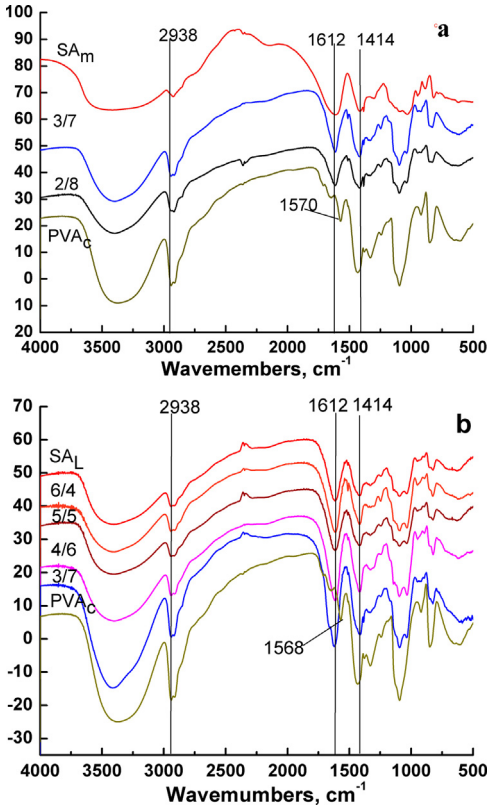

Fig. 4. FTIR-kBr of crude SA, electrospun PVA (8%) and fiber mats electrospun from aqueous mixtures at varied SA/PVA ratios: (a) 3/7, 2/8 SA_m/PVA (5%); (b) 6/4 (6.15%), 5/5 (7.0%), 4/6 (7.8%), 3/7 (5%) SA_l/PVA.

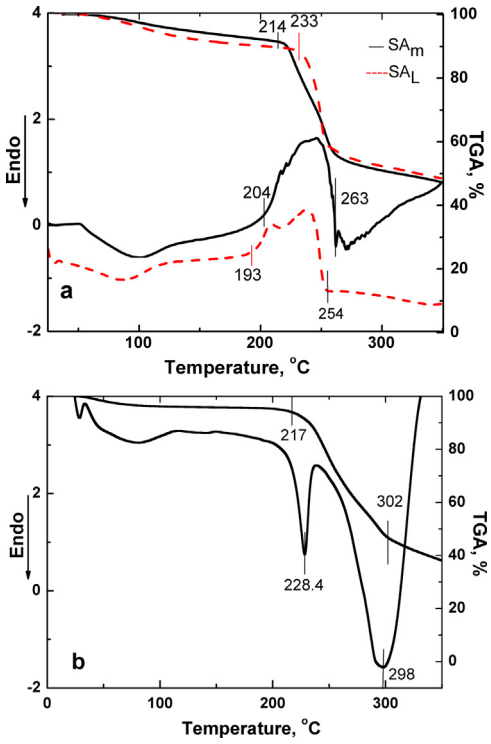

Fig. 5. DSC and TGA of SA and PVA from aqueous solutions (%): (a) SA_m and SA_l cast films (2%); (b) electrospun PVA fibers (8%).

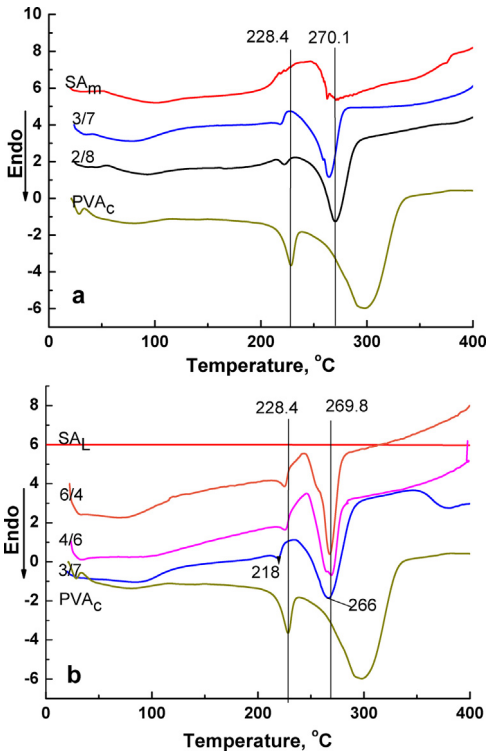

Fig. 6. DSC of SA film cast from 2% aqueous solution, fibers electrospun from aqueous PVA (8%) and mixtures at: (a) 3/7 and 2/8 SA_m/PVA (5%); (b) 6/4 SA_l/PVA (6.15%), 4/6 SA_l/PVA (7.8%), 3/7 SA_l/PVA (5%).

Ca^{2+} cations individually as well as together in the electrospun 3/7 SA_l/PVA fibers were studied.

3.5.1. Cross-linking of PVA fibers

The as-spun PVA fibers turned clear upon contacting water and dissolved partly after 2 h, losing 64.8% weight. Immersing PVA fibers in 95% ethanol either for 24 h or 10 min five times with drying (65 °C, 15 min) in between reduced mass loss considerably to 6.9% (24 h) or 9.7% (10 min, 5 times), respectively. Following water immersion for 2 h, these ethanol exchanged PVA fibers lost additional 9.4% (24 h) and 14.8% (10 min, 5 times) mass, totaling 16.9% and 25.9% from the original, respectively. A single 24 h ethanol exchange led to 9% less mass loss or reduced water solubility of PVA fibers to a greater extent, thus more favorable.

Ethanol exchange, by either process, eliminated the moisture peak in PVA fibers, showing successful moisture exchange, while also raised the PVA melting temperature from 228 °C to 233 °C and heat from 36.8 J/g to 50.2 J/g (10 min for 5 times) and 63.4 (24 h) (Fig. 7a). These improved melting behaviors are clear indication of larger crystal sizes and/or increased crystallinity, contributing to their improved stability in water.

3.5.2. Cross-linking of SA

The as-cast SA_m film swelled then dissolved in water in a minute and was not altered after five repetitive 10-min ethanol exchanges as expected. Immersion in 2% $CaCl_2$ (75% ethanol) for 30 min and 2 h, only lengthened the time taken to dissolve to 10 min and 12 min, respectively. Immersion in a higher 5% $CaCl_2$ concentration for 30 min rendered the film insoluble in water for up to 2 h. SA_m film first gained 15% weight from 5% $CaCl_2$–ethanol immersion, partially from Ca^{2+} intake, then lost 14.6% after 1-min water washing, finally losing 27.8% after 2 h water immersion, all mass being cummalative based on original. No further weight loss was observed after extended water immersion for 4 h. These observations showed

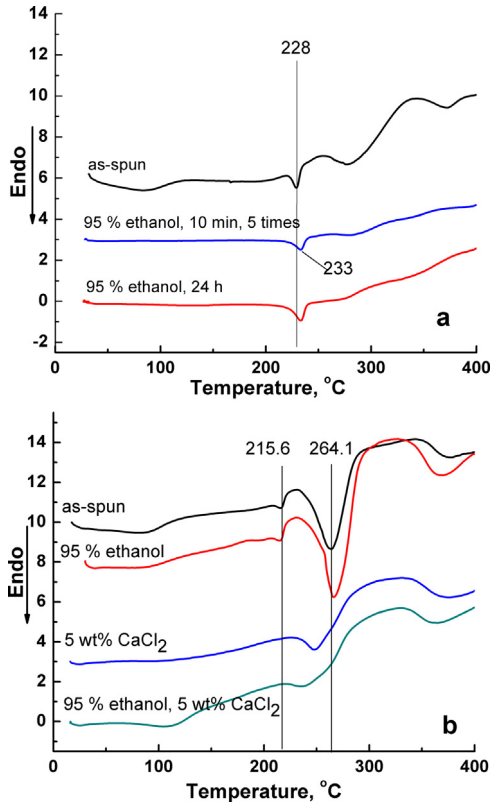

Fig. 7. DSC of as-spun and crosslinked electrospun fibers: (a) PVA (8%), (b) 3/7 SA_l/PVA (5%).

that SA_m film were substantially cross-linked by exchanging the monovalent sodium with bivalent calcium in a 30 min immersion with 5% $CaCl_2$ in 75% ethanol.

3.5.3. *Cross-linking of 3/7 SA_l/PVA fiber mat*

The 3/7 SA_l/PVA hybrid fibers were exchanged with ethanol alone as well as $CaCl_2$–ethanol at varied $CaCl_2$ and ethanol concentrations for varied lengths of time. The original 3/7 SA_l/PVA mat fell apart into pieces in less than 1 min. The ethanol exchanged 3/7 SA_l/PVA fibers (95%, five 10-min repetitions) remained insoluble after 2 h water immersion, but lost 34.6% mass. Assuming ethanol exerting the same effect on PVA in these fibers, dissolution of PVA would lead to 18.1% mass loss based on the 25.9% weight loss from PVA fibers under the same condition. The 16.5% extra mass loss from the hybrid fibers would then be from the dissolution of SA_l, meaning not all 30% of SA_l in the fibers was soluble. As ethanol exchange was not expected to affect the solubility of SA as confirmed experimentally and described earlier, the reduced solubility of SA_l in the hybrid fibers might be due to the increased crystallinity of PVA domains which trap and/or bound SA within the fibers, reducing its solubility and/or reduced water accessibility to SA in the fibers.

The 3/7 SA_l/PVA fibers were then exchanged with $CaCl_2$ under various conditions. Exchanged with 5 and 8% $CaCl_2$ in 75% ethanol (10 min, 5 times) improved the stability of these hybrid fibers in water, losing 6.8% and 12% mass after 2 h immersion. Neither increasing ethanol concentration to 95% nor lengthening exchange time to 2 h at constant 8% $CaCl_2$ could improve the stability of these fibers in water but, in fact, cause considerable mass losses of 22.3% and 16.4%, respectively. Stepwise cross-linking in 95% ethanol for 20 min, followed by 20 min 5% $CaCl_2$ (75% ethanol) immersion also did not improve their water stability, losing 18.3% weight. These might be due to the reduced solubility of $CaCl_2$ in 95% ethanol and dissolution of SA under prolonging exposure to the aqueous environment.

In cross-linking by ionic exchange, the mass gained in the first 10 min was attributed to the uptake of Ca^{2+} as well as the solvents. The weight loss following the exchange could be explained by loss of the displaced Na^+ and residual free Ca^{2+} as well as partial dissolution of SA_l/PVA fibers. The optimal cross-linking to render fibers stable in water was 5% $CaCl_2$ (75% EtOH, 30 min). The so-crosslinked SA_l/PVA fibers lost 6.8% after 2 h water immersion.

Ethanol exchange (95%, 20 min) imposed very little change to the thermal behavior of 3/7 SA_l/PVA fibers (Fig. 7b). The small PVA melting peak at 216 °C remained unchanged while PVA decomposition peak increased slightly from 264 °C to 266 °C and heat of decomposition lowered substantially from 985 J/g to 654 J/g, indicating that ethanol exchange did not affect the original PVA crystalline structure but slightly altered the overall decomposition of SA_l/PVA. Exchange with $CaCl_2$ (5% in 75% ethanol, 30 min), on the other hand, caused the PVA melting and decomposition peaks to disappear completely while a new endotherm emerged at 248 °C, between the melting and decomposition peaks of PVA. The new peak had a heat of 216 J/g, much higher than the melting heat of PVA (36.8 J/g), suggesting that dehydration and ionic links among SA chains affect not only the crystalline PVA domains, but also both PVA and SA in the hybrid fibers. Likewise, the two-step ethanol (95%, 20 min) and 5% $CaCl_2$ (75% ethanol, 20 min) also caused the PVA melting and decomposition peaks to disappear, but the new endotherm had a much smaller heat of 131 J/g and a lower temperature, again affirming the 5% $CaCl_2$ (75% EtOH, 30 min) to be more effective in crosslinking.

4. Conclusion

Sodium alginates (SA) dissolved in water readily, but their aqueous solutions gelled at low concentrations, i.e., 4% for SA_m and 8% for SA_l, making them impossible to be electrospun alone into fibers. Thorough studies of the viscosity behaviors of aqueous SA/PVA mixtures gave evidence to how the abundant SA–PVA as well as PVA–PVA intermolecular hydrogen bonds could balance SA–SA repulsion to provide necessary chain entanglement to support robust electrospinning into uniform fibers. With increasing SA contents, SA–SA repulsion first balanced then exceeded the intermolecular SA–PVA and PVA–PVA hydrogen bonding to lower overall viscosity, enabling fiber spinning. Solution viscosities could thus be tuned by SA/PVA ratios and total concentrations to permit robust and continuous electrospinnning of aqueous mixtures of low viscosity SA_l (50 mPa s at 1%) and medium viscosity SA_m (300 mPa s at 1%) at up 33.3% and 60% alginate contents, respectively. SA_l/PVA mixtures with 33.3% to 60% SA_l had viscosities ranging from 530 to 3600 mPa s and could be electrospun continuously for at least 48 h. The most uniform fibers were obtained at 2/8 (w/w) SA_m/PVA ratio with diameters from 153 nm to 260 nm and 3/7 (w/w) SA_l/PVA with 140 nm to 350 nm diameters. While intermolecular SA–PVA hydrogen bonding in the mixtures and hybrid fibers were evident from their viscosities and FTIR, some phase separation of both SA and PVA in the hybrid fibers was also indicated by their thermal behaviors. The hybrid fibers were rendered water insoluble by crosslinking with 5% $CaCl_2$ in75% EtOH for 30 min, i.e., simultaneous cationic crosslinking of SA and ethanol exchange induced crystallization of PVA. These findings demonstrated a green approach involving aqueous electrospinning and physical crosslinking to create biologically compatible and ingestible alginate hybrid fibers for potential biomedical, food and other applications.

Appendix A. Supplementary data

Supplementary data associated with this article can be found, in the online version, at http://dx.doi.org/10.1016/j.carbpol.2013.10.066.

References

Alborzi, S., Lim, L.-T., & Kakuda, Y. (2010). Electrospinning of sodium alginate–pectin ultrafine fibers. *Journal of Food Science*, *75*(1), C100–C107.

Bhattarai, N., Li, Z., Edmondson, D., & Zhang, M. (2006). Alginate-based nanofibrous scaffolds: Structural, mechanical, and biological properties. *Advanced Materials*, *18*(11), 1463–1467.

Bonino, C. A., Krebs, M. D., Saquing, C. D., Jeong, S. I., Shearer, K. L., Alsberg, E., et al. (2011). Electrospinning alginate-based nanofibers: From blends to crosslinked low molecular weight alginate-only systems. *Carbohydrate Polymers*, *85*(1), 111–119.

de Gennes, P. G. (1979). *Scaling concepts in polymer physics*. Ithaca, NY: Cornell University Press.

Donati, I., & Paoletti, S. (2009). Material properties of alginates. In B. H. A. Rehm (Ed.), *Alginates: Biology and applications* (pp. 1–53). Berlin/Heidelberg: Springer.

Islam, M. S., & Karim, M. R. (2010). Fabrication and characterization of poly(vinyl alcohol)/alginate blend nanofibers by electrospinning method. *Colloids and Surfaces A: Physicochemical and Engineering Aspects*, *366*(1–3), 135–140.

Kong, Q. S., Yu, Z. S., Ji, Q., & Xia, Y. Z. (2009). Electrospinning of sodium alginate with poly(ethylene oxide), gelatin and nanometer silver colloid. *Materials Science Forum*, *610–613*, 1188–1191.

Lee, Y. J., & Lyoo, W. S. (2009). Preparation and characterization of high-molecular-weight atactic poly(vinyl alcohol)/sodium alginate/silver nanocomposite by electrospinning. *Journal of Polymer Science Part B: Polymer Physics*, *47*(19), 1916–1926.

Lee, Y. J., Shin, D. S., Kwon, O. W., Park, W. H., Choi, H. G., Lee, Y. R., et al. (2007). Preparation of atactic poly(vinyl alcohol)/sodium alginate blend nanowebs by electrospinning. *Journal of Applied Polymer Science*, *106*(2), 1337–1342.

Lu, J.-W., Zhu, Y.-L., Guo, Z.-X., Hu, P., & Yu, J. (2006). Electrospinning of sodium alginate with poly(ethylene oxide). *Polymer*, *47*(23), 8026–8031.

Ma, G., Fang, D., Liu, Y., Zhu, X., & Nie, J. (2012). Electrospun sodium alginate/poly(ethylene oxide) core–shell nanofibers scaffolds potential for tissue engineering applications. *Carbohydrate Polymers*, *87*(1), 737–743.

Nie, H., He, A., Wu, W., Zheng, J., Xu, S., Li, J., et al. (2009). Effect of poly(ethylene oxide) with different molecular weights on the electrospinnability of sodium alginate. *Polymer*, *50*(20), 4926–4934.

Nie, H., He, A., Zheng, J., Xu, S., Li, J., & Han, C. C. (2008). Effects of chain conformation and entanglement on the electrospinning of pure alginate. *Biomacromolecules*, *9*(5), 1362–1365.

Qin, Y. (2004). Gel swelling properties of alginate fibers. *Journal of Applied Polymer Science*, *91*(3), 1641–1645.

Rhim, J.-W. (2004). Physical and mechanical properties of water resistant sodium alginate films. *LWT-Food Science and Technology*, *37*(3), 323–330.

Safi, S., Morshed, M., Hosseini Ravandi, S. A., & Ghiaci, M. (2007). Study of electrospinning of sodium alginate, blended solutions of sodium alginate/poly(vinyl alcohol) and sodium alginate/poly(ethylene oxide). *Journal of Applied Polymer Science*, *104*(5), 3245–3255.

Shalumon, K. T., Anulekha, K. H., Nair, S. V., Nair, S. V., Chennazhi, K. P., & Jayakumar, R. (2011). Sodium alginate/poly(vinyl alcohol)/nano ZnO composite nanofibers for antibacterial wound dressings. *International Journal of Biological Macromolecules*, *49*(3), 247–254.

Zhang, N. B. A. M. (2007). Controlled synthesis and structural stability of alginate-based nanofibers. *Nanotechnology*, *18*(45)